

TECHNIQUE FOR GENERATION OF UNIPOLAR ULTRASONIC PULSES

D. O. Thompson and D. K. Hsu

Ames Laboratory, USDOE
Iowa State University
Ames, IA 50011

INTRODUCTION

Substantial progress has been made in recent years in the development of inverse elastic wave scattering theories for use in ultrasonic nondestructive evaluation (NDE). These include theories that are applicable in different ultrasonic frequency ranges and include formulations in various approximations [1-15]. It is by application of these inverse scattering solutions to ultrasonic inspection results that quantitative measures of the size, shape, and orientation of a flaw can be determined.

Implementation of the inverse scattering solutions mentioned above, however, has been limited. One of the principal reasons for this limitation is the narrow bandwidth of commercial ultrasonic instrumentation relative to the ultrasonic bandwidths needed to properly employ the inverse results over a range of flaw sizes. Addison et al. [16] have shown that the minimum bandwidth needed to size a flaw with radius a using the simplest, 1-D inverse Born scattering solution must extend from $ka=0.5$ to $ka=2.0$ to achieve sizing accuracies of 20%. k is the magnitude of the wave vector and is given by $2\pi/\lambda$ where λ is the ultrasonic wavelength. This requirement is considerably more demanding than the capabilities of most commercially available transducers. Addison et al. also showed that inattention to this specification will result in size estimates that are either too small or too large depending upon whether there is a deficiency of the low or high frequency content in the interrogating ultrasonic spectrum.

In order to utilize the inverse theories and to accommodate a reasonable range of flaw sizes that are unknown to the investigator, it is evident that considerable improvement in ultrasonic system bandwidths must be obtained. Unipolar pulses provide an attractive way to approach this objective. Features of this pulse have been described by a number of authors [17,18,19]. Current practice, however, seems to be limited to the pitch-catch mode. In this configuration one transducer is connected to a low impedance electronic pulser and is used to transmit the signal while a second transducer is connected to a high impedance amplifier and is used to receive the signal. This configuration, however, is much too limited for NDE applications in which the preponderance of applications requires the pulse-echo mode in which the same transducer is used for transmitting and receiving.

The purpose of this paper is to report results that describe a new way to generate broadband, unipolar pulses in pulse-echo operation using conventional planar transducers. A review of requirements is first given; this summary is then followed by a description of a transmit/receive switch that has been developed for pulse-echo operation and some results that have been obtained with it. These results are then discussed and compared with results obtained with conventional instrumentation.

EXPERIMENTAL PROCEDURE

Review of Requirements

The production of broadband, unipolar stress pulses using a piezoelectric generator in a pulse-echo mode requires consideration of both the transmit and receive aspects of the process. It is well known [20] that a step function voltage pulse applied to an untuned planar piezoelectric transducer with perfectly matched backing will produce a unipolar stress pulse that shows similarities to, but in fact is not, the time derivative of the applied voltage pulse. The "effective" differential character arises because the charge layers produced on opposite faces of the piezoelectric by the applied voltage pulse produce stress pulses that are replicas of the pulse, but which are of opposite polarities and which are separated in time by an amount equal to one transit time through the piezoelectric. In the receive mode, the piezoelectric transducer generates a voltage signal that faithfully represents the unipolar stress pulse under open circuit (no load) conditions. However, the features of this reproduction are modified considerably by values of the parameter $R_L C_0 \omega$ in which R_L is the impedance of the external circuit used to measure the signal, and $C_0 \omega$ is the reciprocal of the transducer source impedance. If $R_L C_0 \omega \ll 1$, it follows that the open circuit voltage signal is differentiated by the measuring circuit, whereas if $R_L C_0 \omega \gg 1$, the measuring circuit does not significantly perturb the open circuit signal generated by the piezoelectric. In the latter case, then, the received signal will also appear as a unipolar pulse.

Examples of the discussion given in the previous paragraph are given schematically in Fig. 1 for two different applied voltage pulses and for both the transmit and receive modes. Figure 1a shows that the expected transmitted stress pulse is unipolar if the applied voltage pulse is a step function, and that the measured, or received, signal is either unipolar or bipolar depending upon whether $R_L C_0 \omega \gg 1$ or $R_L C_0 \omega \ll 1$. Figure 1b shows the expected behavior for the transmitted and received pulse for the commonly used spike applied voltage pulse. In this case the stress pulse is bipolar, and depending again upon the relative values of $R_L C_0 \omega$, the received pulse is either bipolar if $R_L C_0 \omega \gg 1$ or the commonly observed tripolar pulse if $R_L C_0 \omega \ll 1$. It should be emphasized that this figure is only schematic; the actual shape of the unipolar stress pulse is expected to vary according to the rise time of the applied voltage pulse and the transit time of the back surface stress pulse through the piezoelectric. Furthermore, the idealized examples assume that there are no diffraction or frequency dependent attenuation losses associated with pulse propagation that would tend to distort the shapes of both the stress pulses and the received signals when viewed in the time domain.

Transmit/Receive Switch

From the above descriptions, it is clear that a special transmit-receive switch is needed in order to generate and receive unipolar pulses in a pulse-echo mode. The switch must provide a way to connect

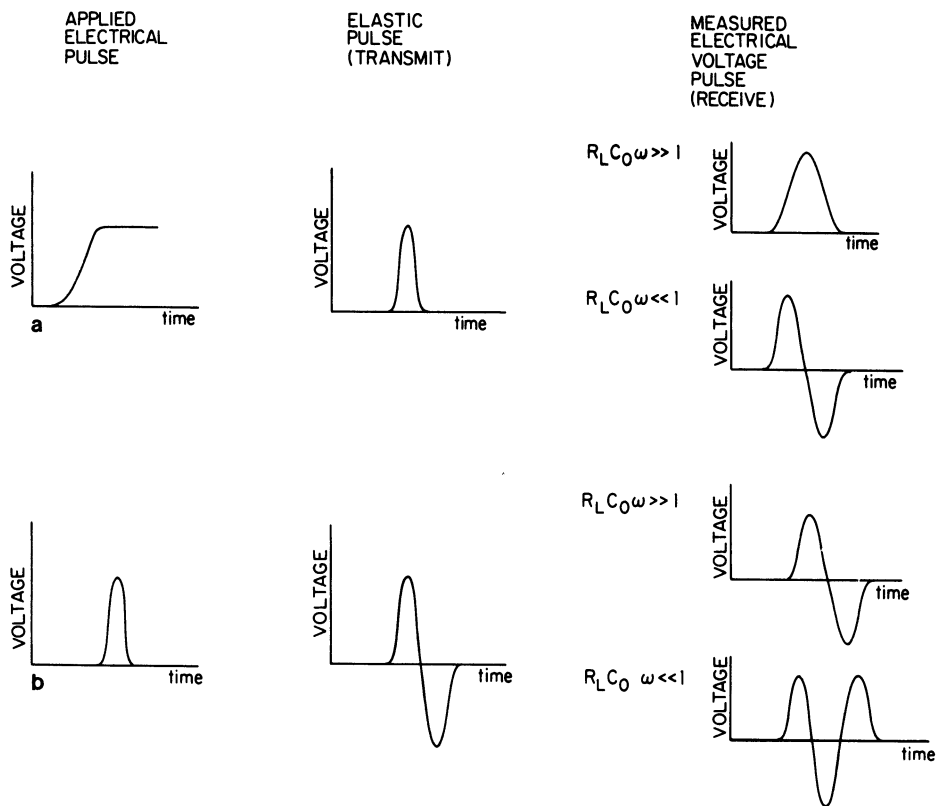


Fig. 1. Transmitted and received pulse shapes for both a step function excitation voltage and a spike excitation voltage.

the transducer electronically to a low impedance applied voltage pulser during the transmit cycle and to a receiver with high input impedance during the receive cycle. Figure 2 shows a recently developed transmit-receive switch that has these properties. The low impedance pulsing transmitter is shown at the left, the transducer T with internal impedance $1/jC_0\omega$ in the center, and an FET with high input impedance and low output impedance on the right. R_1 is nonessential to the operation of the circuit for single transducer operation. It is included because the circuit is used in a multiplexing mode in which the transmitter is switched electronically to alternate transducers [21]. The only purpose of this resistance is to keep the circuit input at ground potential when the transmitter is switched to other circuits. The diodes D_1 provide a low impedance conducting path during the transmit cycle of the pulser. During the receive cycle of the pulse echo mode, these diodes effectively block the low impedance transmitter from the transducer because of the relatively low signal levels. The inclusion of the diodes D_1 is therefore essential since the impedance in all current paths from the transducer must be included in the calculation of the load impedance R_L presented to the transducer. Diodes D_2 are included as a protective device to shield the FET (or following preamplifier) from the "main bang" of the transmitter. Resistor R_2 is included as a parallel load resistor for the transducer so that the diodes D_2 do not simply short the main transmitter pulse to ground during the transmit cycle. A value of $R_2 = 270\Omega$ has been used to date. This value is not critical, but must be several times larger than the input impedance of the transducer for all operating frequencies. Received signals in the pulse echo mode are coupled to the high impedance FET through the network R_3C_1 . Two conditions apply to the choice of these values although, as before, the actual values are not very critical. In one

of these the R_3C_1 value is selected to produce the desired time constant and to set the low frequency end of the signal pass band. In the case shown, the time constant is $2.4\mu\text{sec}$ with a low frequency pass limit of 0.4MHz . Secondly, the impedance of this network should be chosen so that the total load impedance presented to the transducer is 10-20 times the source impedance of the transducer. Since the diodes are essentially nonconducting in the receive mode and the FET possesses a very large input impedance, the only substantive contributors to the transducer load impedance are R_2 , C_1 , and R_3 . A value for $R_3=10\text{K}$ ohms has been found satisfactory for work to date. The transmit-receive switch is completed with an FET buffer that is connected to a following broadband preamplifier (Comlinear). The values of resistances used in the FET produce an output impedance of about 120Ω . Lower output impedances can be obtained using other values for R_4 and R_5 . It should be noted that the use of an FET is optional and depends upon circuit arrangements of the following electronics.

Results

The transmit-receive switch described in the previous section has been used to generate unipolar pulses with standard, commercially available piezoelectric transducers. All results given in this section were obtained using a water immersion technique and a flat metal reflector that could be placed at prescribed distances from the transducer. Panametrics transducers with 10 and 15 MHz center frequencies and $1/4$ inch diameters were used. It is important that the transducers contain only an internal piezoelectric element and no internal tuning elements. The voltage pulses applied to the transducers were step function pulses generated by a Hewlett Packard 214A generator. After reflection from the metallic reflector, received signals were taken from the transmit-receive

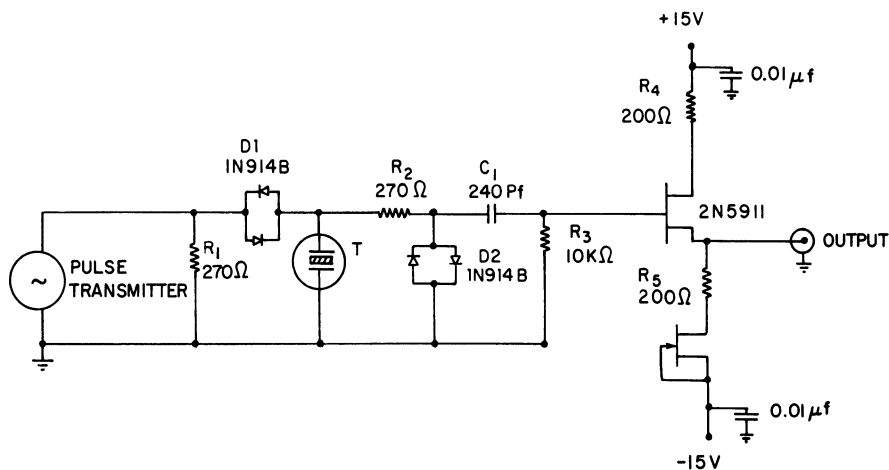


Fig. 2. Schematic circuit diagram for the transmit-receive switch used in producing the unipolar ultrasonic pulse.

switch shown in Fig. 2, amplified in a Comlinear preamplifier with 3dB points at 0 and 150 MHz, digitized in a Tektronix 7912 A/D converter, and displayed. Results were obtained using the transmit-receive switch both with and without the FET buffer.

Figures 3a and 3b show results obtained for the 10 MHz, 1/4 inch, immersion transducer in which the FET buffer in the transmit-receive switch was included. Figure 3a shows the received time domain pulses taken at several distances between the transducer face and the metallic reflector, and Fig. 3b shows the spectral analysis of the time domain pulses at the same distances. The results in Fig. 3a show that, at close distances, acceptable unipolar pulses are produced, and that with increasing separation, the unipolar pulse degrades toward bipolar behavior. The small, sharper spikes on the positive side of the negative-going pulse appear to be associated with internal reverberations in the piezoelectric due to imperfect backing. It would appear from the results in Fig. 3b that the unipolar degradation observed in Fig. 3a is due to the loss of low frequency content because of diffraction. The results in Fig. 3b also show the signal enhancement at 10MHz due to the quarter wave plate that is present in the immersion transducers.

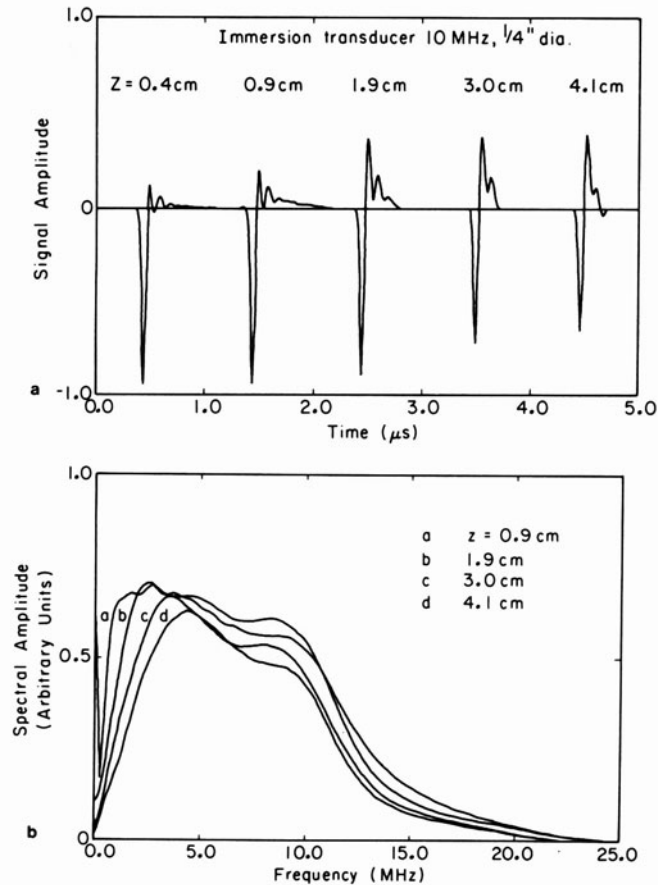


Fig. 3. a) Received ultrasonic pulses in the pulse-echo mode at various transducer-reflector distances using a 10 MHz, 1/4 inch diameter immersion transducer and with the FET in Fig. 2 included.
 b) Frequency spectra of the ultrasonic pulses shown in Fig. 3a.

The frequency spectra obtained for a contact transducer used in an immersion mode are shown in Fig. 4a. Even though this transducer is not intended for immersion applications and does not possess a matching quarter wave plate, the omission of this plate does not appreciably affect the generation of the unipolar pulse. The results shown in Figs. 3b and 4b show a degradation in the low frequency content of the unipolar pulse signal with separation between the transducer and the reflecting plate. As noted, this effect is to be expected in terms of diffraction losses. If this be true, application of diffraction corrections to the various frequency spectra should reduce all the spectral results to a common curve for a particular transducer. Figure 4b shows the results obtained when diffraction corrections are applied to the results of Fig. 4a. It will be seen that a universal curve results which is the true spectral response of the transducer for the applied voltage step function condition. Similar results have been obtained for all the other cases examined.

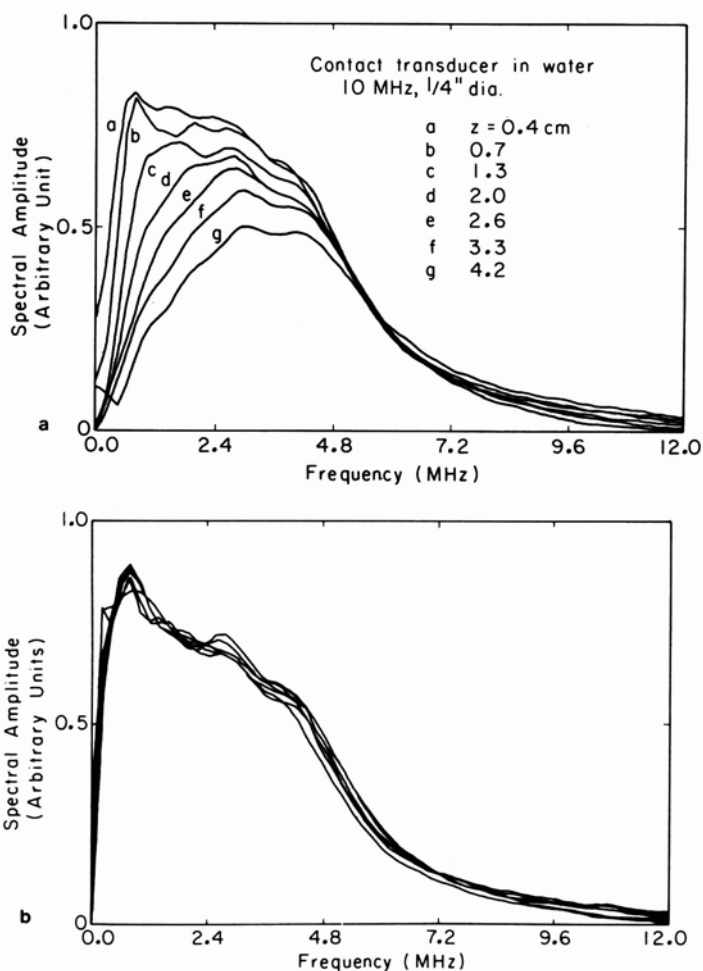


Fig 4. a) Frequency spectra of ultrasonic pulses in the pulse-echo mode at various transducer-reflector distances using a 10MHz, 1/4 inch contact transducer in the immersion mode. The FET buffer in the transmit-receive switch is bypassed. b) Intrinsic frequency spectrum of the unipolar pulse obtained by applying diffraction corrections to the spectra in Fig. 4(a).

Although it is possible to correct analytically for diffraction losses as shown above, the corrections do not restore lost energy into the interrogating ultrasonic beam. A principal consequence of this loss is a degraded signal/noise ratio at the lower end of the frequency spectrum. Considerations are in progress aimed at reducing the diffraction losses through the use of long focal length lenses. Figure 5 shows the results obtained using a plane wave, 15 MHz, 1/4 inch transducer both with and without a 69 centimeter focal length lens. The lens in this case was cast from epoxy to the desired radius of curvature and then cut to an edge thickness of 0.012 inches using a diamond saw. For test purposes, the lens was bonded to the transducer face with glycerin. The top part of the figure shows spectral results obtained at three separations with no lens and the bottom part shows the same results with the lens in place. It is evident that the lens action helps to provide beam collimation and suppression of diffraction losses in this case. Further studies to select a more ideal collimating lens are in progress.

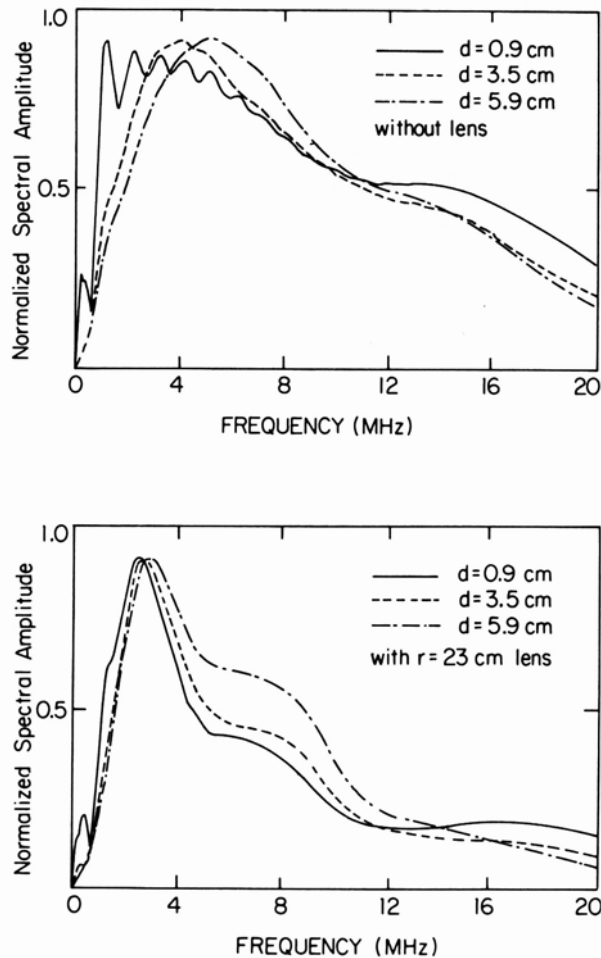


Fig. 5. Frequency spectra of ultrasonic pulse-echo signals at three transducer-reflector distances with the 69cm focal length lens (bottom figure) and without the lens (top figure). The spectra are normalized to have the same peak value. The transducer is a 15 MHz, 1/4 inch diameter immersion transducer.

DISCUSSION OF RESULTS

As noted in the Introduction, one of the principal purposes of this work was to develop a convenient way to obtain broadband ultrasonic pulses that can be used with pulse-echo measurement techniques and with a variety of more or less standard transducers. The transmit-receive switch that has been developed appears to satisfy this purpose. It can be assembled and used separately or it can easily be incorporated into existent voltage pulser units. Two limitations have been found that need to be noted. First, the transducer used must not contain an inductive tuning element and secondly, the applied voltage pulser used as a driver must be capable of providing sufficient current so that the step function pulse applied to the transducer is sharply formed. Further, it has been found that the top frequency limit of the transducer's bandwidth in this mode of operation is effectively defined by the high frequency roll off of the piezoelectric resonance. The low frequency pass band limit is determined by the values of components in the transmit receive switch.

The magnitude of the transducer bandwidth improvement obtained with the current transmit-receive switch is shown in Fig. 6. Curves are shown in this figure for the pulse echo response of another 10MHz, 1/4 inch immersion transducer with the reflector placed at 6 cm from the transducer and for four different values for the resistance R_3 shown in Fig. 2. The values for the resistance are 50Ω , 390Ω , $10K\Omega$, and $47K\Omega$ for curves 1, 2, 3, and 4, respectively. No diffraction corrections have been applied to these results. It is apparent that the improvement in bandwidth is very significant across this range. It is also apparent that increases in R_3 above $10K\Omega$ produce only small changes in the overall bandwidth and at the expense of lengthened time constants.

One of the tests that must be applied to the extended bandwidth transducer as an indicator of its flaw sizing capability is to compare the measured scattering amplitude with theoretical predictions for a well-defined ultrasonic target. Such a comparison is shown in Fig. 7 for a machined ellipsoidal void that was diffusion bonded in a titanium block.

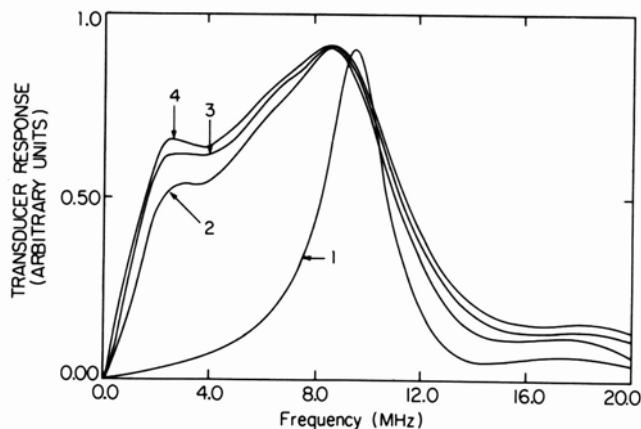


Fig. 6. Frequency spectra of a 10 MHz, 1/4 inch diameter immersion transducer placed 6 cm from a flat reflector and operated in the pulse-echo mode using the transmit-receive switch of Fig. 2. Curves 1, 2, 3, and 4 correspond, respectively, to $R_3=50$, 390 , $10K$, and $47K\Omega$.

The ellipsoidal void was oblate in shape, and the nominal values of the semiaxes were 400μ , 400μ and 200μ . Opsal [22] has calculated the scattering amplitude for this target; his results are given by the dashed line. The solid curve shows the experimental results obtained using the unipolar pulse in the pulse-echo mode. These curves are given in absolute units and include diffraction and attenuation corrections. The agreement between the curves is considered very satisfactory. It is evident that it would have not been possible to obtain results that agree this well with theoretical predictions had the low impedance response curve of Fig. 6 been used.

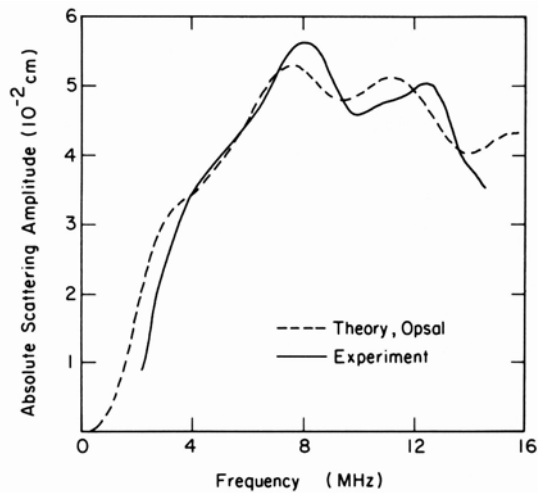


Fig. 7. Absolute scattering amplitude of an oblate spheroidal cavity in titanium with semiaxes of 400μ and 200μ . The dashed curve is the theory and the solid curve is the experimental result obtained with the unipolar pulse in the pulse-echo mode.

ACKNOWLEDGEMENT

The Ames Laboratory is operated for the U.S. Department of Energy by Iowa State University under Contract No. W-7405-ENG-82. This work was supported by the Director of Energy Research, Office of Basic Energy Sciences.

REFERENCES

1. J. M. Richardson, in 1978 Ultrasonics Symposium Proceedings (IEEE, New York, 1978), pp. 759-766.
2. W. Kohn and J. R. Rice, *J. Appl. Phys.* 50, 3353 (1979).
3. J. E. Gubernatis, J. A. Krumhansl, and R. M. Thomson, *J. Appl. Phys.* 50, 3338 (1979).
4. J. E. Gubernatis and E. Domany, *J. Appl. Phys.*, 50, 818 (1979).
5. B. Budianski and J. R. Rice, *J. Appl. Mech.* 45, 453 (1978).
6. M. T. Resch, J. C. Shyne, G. S. Kino, and D. V. Nelson, in Review of Progress in Quantitative NDE 1, D. O. Thompson and D. E. Chimenti, Eds., (Plenum Press, NY, 1982), p. 573.
7. B. T. Khuri-Yakub, G. S. Kino, K. Liang, J. Tien, C. H. Choa, A. G. Evans, and D. B. Marshall, Ref. 6, p. 601.
8. J. M. Richardson and K. Fertig, in Proceedings DARPA/AF Review of Progress in Quantitative NDE, AFWAL-TR-80-4078 (1980), p. 528.
9. J. M. Richardson, in Proceedings DARPA/AFML Review of Progress in QNDE, AFML-TR-78-205 (1979), pp. 332 and 340.
10. N. Bleistein and J. K. Cohen, in Proceedings DARPA/AFML Review of Progress in QNDE, AFML-TR-78-55 (1978), pp. 73-80.
11. J. H. Rose and J. A. Krumhansl, *J. Appl. Phys.* 50, 2951 (1979).
12. E. Domany, K. E. Newman, and S. Teitel, in Proceedings DARPA/AFML Review of Quantitative NDE, AFWAL-TR80-4078 (1979), p. 341.
13. J. H. Rose and J. L. Opsal, in Review of Progress in Quantitative NDE 1, D. O. Thompson and D. E. Chimenti, Eds., (Plenum Press, NY, 1982), p. 573.
14. V. G. Kogan and J. H. Rose, in Review of Progress in Quantitative NDE 2, D. O. Thompson and D. E. Chimenti, Eds., (Plenum Press, NY, 1983), p. 1141.
15. J. H. Rose, R. K. Elsley, B. R. Tittman, V. V. Varadan, and V. K. Varadan, in Acoustic, Electromagnetic, and Elastic Wave Scatteirng--Focus on the T-Matrix Approach, V. K. Varadan and V. V. Varadan, Eds., (Pergamon, NY, 1980), p. 605.
16. R. C. Addison, R. K. Elsley, and J. F. Martin, in Review of Progress in QNDE, 1, D. O. Thompson and D. E. Chimenti, Eds., (Plenum Press, NY, 1982), pp. 251-261.
17. F. Yu, D. B. Ilic, B. T. Khuri-Yakub, and G. S. Kino, in IEEE Ultrasonic Symposium Proceedings, 1979, pp. 284-288.
18. R. B. Thompson, K. M. Lakin, and J. H. Rose, in IEEE Ultrasonics Symposium Proceedings, 1981, pp. 930-935.
19. J. F. Muratore, H. R. Carleton, and H. Austerlitz, in IEEE Ultrasonics Symposium Proceedings, 1982, pp. 1049-1053.
20. B. A. Auld, Acoustic Fields and Waves in Solids, Vol. 1, (Wiley, 1973).
21. D. O. Thompson and S. J. Wormley, in Review of Progress in QNDE, 4, D. O. Thompson and D. E. Chimenti, Eds., (Plenum Press, NY, 1984), pp. 287-296.
22. J. L. Opsal, *J. Appl. Phys.* 58, 1102 (1985).